EPJ Web of Conferences **308**, 06002 (2024) https://doi.org/10.1051/epjconf/202430806002
ISRD 17

On radiation situation in vicinity of PET production cyclotron

Marek Zmeškal[1,*], *Michal* Košťál[1,**], *Tomáš* Czakoj[1], *Jan* Šimon[1], *Martin* Schulc[1], *Šimon* Vadják[2], *Michal* Antoš[2], and *Zdeněk* Matěj[3,***]

[1]Research Centre Rez, Hlavni 130, 250 68 Husinec-Rez, Czech Republic
[2]UJV Rez, Hlavni 130, 250 68 Husinec-Rez, Czech Republic
[3]Masaryk University, Botanická 15, 612 00 Brno, Czech Republic

Abstract. The medical cyclotrons intended for the production of medical isotopes are relatively widespread. The most common radioisotope product of these facilities is ^{18}F which origins from ^{18}O(p, n)^{18}F reaction. Due to relatively large amounts of produced nuclei, the leakage neutron and gamma flux is a big issue in radiation safety in such cyclotron labs. Due to relatively high energies of accelerated protons, high energy gammas and neutrons are produced with energies above 10 MeV with high penetration properties. Neutron and gamma spectra around cyclotron IBA Cyclone 18/9 intended for production of ^{18}F was measured with stilbene detector. It was compared to simulated neutron spectra with various Monte Carlo codes and with spectral indices calculated from reaction rates in activation detectors. Strong disagreement in simulation of spectra in backward angles was found for MC codes Geant4 and MCNP6.2.

1 Introduction

Positron emission tomography (PET) is a diagnostic technique designed for imaging metabolic processes. A substance labeled with a radioisotope that undergoes β+ decay must be injected into the patient's body to use this method. The most commonly used radioisotope for PET is fluorine-18. It is most often produced in compact accelerators, which are often located near or inside hospitals. Sufficient shielding must be built around the cyclotron to provide radiation protection, because the cyclotron is source of high energy neutrons and gamma during its operation. In order to optimise this shielding, it is necessary to know the spectrum of these secondary particles. However, knowledge of the neutron spectrum is also important to determine the activation of the structural parts of the cyclotron and the bunker itself. Last but not least, it is also interesting for other potential uses of this radiation, such as validation of cross sections or testing the radiation resistance of electronic components.

This paper deals with the characterization of the neutron/gamma field in common IBA Cyclone 18/9 placed in UJV. Experimental characterization is based on the employment of stilbene scintillation spectrometry together with neutron activation analysis using precisely selected activation foils with reaction insensitive to gamma activation. The activation analysis was used for validation of stilbene characterization.

*e-mail: marek.zmeskal@cvrez.cz
**e-mail: michal.kostal@cvrez.cz
***e-mail: matej.zdenek@mail.muni.cz

Few works dealt with characterisation of neutron spectra around such accelerators with the use of different methods. The neutron spectrum at the same facility around the target was already characterized in [1, 2] by both means of activation detectors and stilbene spectroscopy. In [3–5], the neutron spectrum was measured with Bonner sphere spectroscopy (BSS) using pair of thermoluminiscent detectors (TLD) as neutron detectors. BSS was also used in [6], where ^{3}He filled proportional counter was used as a neutron detector inside the polyethylene Bonner spheres instead of TLD. Another approach is to use neutron activation analysis with a set of activation detectors and unfold the neutron spectrum with a deconvolution code [7, 8]. Both of these methods depend on the initial spectrum guess, which is usually calculated by Monte Carlo codes and neither of these methods give a detailed description of the neutron spectrum in the fast energy region (1 – 20 MeV). This work is mainly aimed at the description of the neutron spectrum in this energy region.

2 Experimental setup and methods

2.1 Cyclotron

Measurements of neutron and gamma spectra were performed on the cyclotron IBA Cyclone 18/9 at UJV Rez. It is usually used for production of ^{18}F with reaction ^{18}O(p,n)^{18}F. The liquid target is made of enriched water to 98 % of ^{18}O and is irradiated with protons of energy 18 MeV. The proton current during production is around 70 μA.

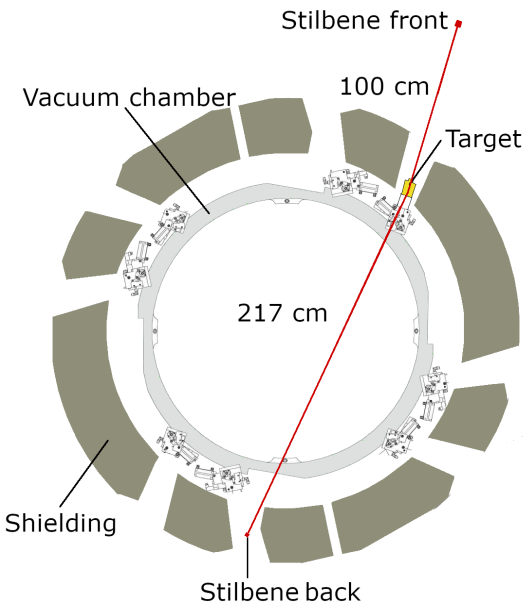

Figure 1. Section of the cyclotron with depicted target and the two positions, where the neutron spectra were measured.

2.2 Stilbene measurement

The fast two-parameter spectrometric system NGA-01 together with active voltage divider was used for the measurements with stilbene scintillator detector (dimensions 10×10 mm for neutron spectra and 45×45 mm for gamma spectra). NGA-01 performs online pulse shape discrimination thanks to a PSD algorithm inside the FPGA chip. Neutron and gamma spectra are then unfolded using the Expectation Maximization algorithm. Response functions for this algorithm were calculated with MCNP6 [9] for gamma photons and our own Monte Carlo transport code for neutrons [10].

Neutron spectrum measurements were performed at two positions around the cyclotron, which are shown in Figure 1. The front measurement was performed at 1 m in a straight line from the proton entry point into the target. The back measurement was made on the other side of the cyclotron in a hole in the shielding for another target. In this way, neutrons could be measured at a reverse angle of about 175° and were shielded almost only by the steel walls of the vacuum chamber. Gamma spectrum measurements were also made at two positions, the first being identical to the location at which the forward neutron spectrum was measured. The second position was approximately 3 m far from the target behind the first concrete shielding.

2.3 Activation detectors

To validate the measured neutron spectra, spectral ratios calculated from different reaction rates in the activation foils were used. These foils were moved to a well-characterised HPGe detector after irradiation. The activities of different radioisotopes and the reaction rates of selected reactions were determined from the intensities of their characteristic gamma lines. The reactions used in the nickel and iron activation foils including their $E_{50\%}$ (energy, which divides integral of the energy dependent reaction rate calculated with measured neutron spectra in front direction in two halves) are shown in the Table 1. One set of activation detectors was placed on the surface of the target collimator at an angle of 168° with respect to the direction of the proton beam and the point of proton entry into the target. The other set was placed at a distance of 1 m from the beginning of the water target in the direct direction in the same point, where the stilbene measurement took place.

Table 1. Used reactions to calculate spectral indices together with their $E_{50\%}$.

reaction	^{nat}Ni(n,x)^{57}Co	^{nat}Ni(n,x)^{58}Co	^{nat}Ni(n,x)^{60}Co	^{nat}Fe(n,x)^{54}Mn
$E_{50\%}$ (MeV)	13	5.9	9.5	6.1

2.4 Simulation

With increasing computational capacity, the possibility of using simulation programs for tasks such as shielding design or activation calculation is also increasing. However, the source term of the secondary neutrons must be correctly described in these programs. Thus, the measured neutron spectrum was also simulated with use of Monte Carlo codes MCNP6.2 and Geant4 [11]. A detailed model of the target and a simplified model of the cyclotron shielding were created in them. For the forward direction, a direct simulation of accelerated protons impinging on the water target was used and the neutron flux was detected at the same location as the scintillator crystal. For the backward direction, a fixed source was created in an external simplified simulation and was then inputted as an energy-angle dependent neutron source in the full simulation. Despite that, the neutrons were detected at a closer position to

the target than where they were actually measured to achieve satisfactory statistical error. The default models, i.e. CEM03.03 in MCNP6.2 and the Bertini cascade model in Geant4, were used in the simulations, although they were intended for simulations of higher energies above 100 MeV. A neutron source using data from the EXFOR database [12] was also created as a fixed source with an energy-angle dependence.

3 Results and discussion

3.1 Neutron spectra

The measured neutron spectrum in the forward direction was normalised to 1 μA and is shown in Figure 2. Since the neutron yields in the different computational models vary, all the results in the forward direction were normalised to a total neutron yield of about $5.2 \cdot 10^{-3}$ neutrons per 1 proton, which was determined from the result in [12] and the average ratio of neutrons above and below 2 MeV. It is substantially higher than the yield of ^{18}F since the neutrons also come from other reactions of protons on ^{18}O [13]. The correctness of this normalisation can be seen by comparing the magnitudes of the individual spectra with the measured one. In addition, it can be seen that Geant4 simulates the shape of the spectrum reasonably well up to about 10 MeV from where it underestimates the spectrum significantly and does not reach to the higher energies above 14 MeV. Because of this observation, an attempt was made to simulate this spectrum with protons of energy 20 MeV instead of 18 MeV (Geant4 20 MeV). It transpired that it simulates the measured spectrum very well (average absolute deviation above 2 MeV is 5.56 %). A very good result is also obtained with a simulation using data from the EXFOR database (average absolute deviation above 2 MeV is 5.46 %). The only shortcomings are a slight overestimation of the highest energies and that the data are only available from 1.7 MeV and therefore there is a strong underestimation for the lowest energies. The data are also only available for 15°. The spectrum simulated by MCNP6.2 then achieves the worst results in shape, overestimating the spectrum below 8.3 MeV and underestimating it above that. On the other hand it is the best simulation in terms of the total neutron yield.

The neutron spectra in backward direction (Figure 3) were normalised above 3 MeV to compare their shapes, because the comparison of the absolute was not possible due to the different location of measurement and simulation. The best agreement is obtained with simulation using data from the EXFOR database, even though they are taken for the 150° angle and so again overestimate the spectra at the highest energies. The Geant4 simulation for the back angles does not match the shape of the spectra even at low and intermediate energies as it did for the forward direction. Instead, it shows similar characteristics to the spectrum simulated by MCNP6.2, overestimating the spectrum below 5.3 MeV and underestimating it for higher energies. However, in a comparison of these two models, the model in Geant4 performs better, reaching to higher energies.

3.2 Spectral indices

Different spectral indices were calculated and are shown in Table 2. Most of them were calculated from reaction rates which were calculated as a product of measured or simulated spectra with cross section taken from IRDFF-II [14] library, except for creation of ^{57}Co, which was combined from IRDFF-II and ENDF\B-VIII.0 [15]. The calculated spectral indices were compared with experimentally determined ones with activation detectors. A very good agreement between stilbene measurement and activation detectors for front spectrum and ^{58}Co/^{57}Co and ^{58}Co/^{54}Mn spectral indices can be seen, which gives us confidence in

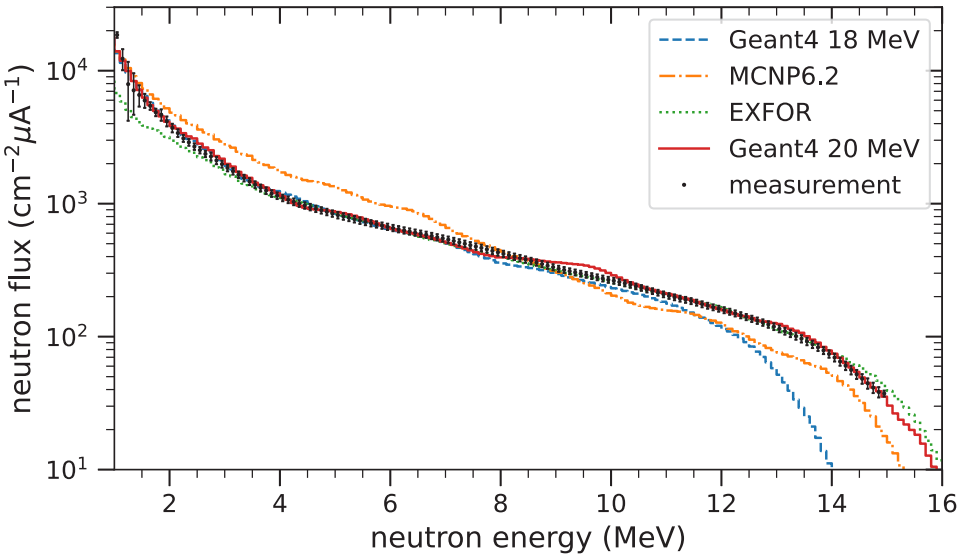

Figure 2. Comparison of neutron spectra at 1 m from the target in front direction calculated in different ways with measured spectra with stilbene detector, all normalised to 1 μA.

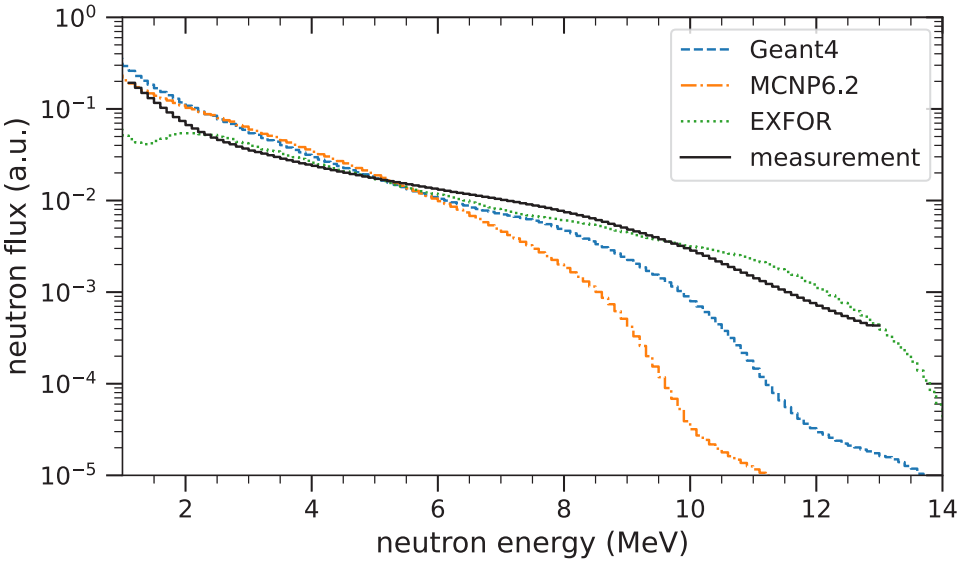

Figure 3. Comparison of neutron spectra emitted to the back calculated with different simulation settings with spectrum measured at the back of the cyclotron, all normalised above 3 MeV.

our measurement. The agreement in the ^{58}Co/^{60}Co spectral index is not so good, which can be caused by uncertainties in the cross section for production of ^{60}Co. The disagreement in spectral indices for back spectra can be mainly caused by different positions of stilbene

measurement and activation detectors. They were placed inside the cyclotron, where a bigger amount of slower neutrons can be present also from other sources such as reaction of protons with collimator. But the phenomenon of decrease of the fast neutrons with increasing angle is confirmed by this measurement.

Table 2. Spectral indices in different places and calculated from different spectra and experimentally determined from activation detectors (AD).

	^{58}Co/^{57}Co		^{58}Co/^{60}Co		^{58}Co/^{54}Mn	
	front	back	front	back	front	back
Geant4	38.9	1312	58.7	136.8	15.3	15.9
MCNP6.2	32.3	14179	66.4	230.8	15.2	15.9
EXFOR	15.6	73.8	47.0	72.9	15.0	15.2
Geant4 20 MeV	17.1	-	48.2	-	15.2	-
stilbene	18.8	130.9	48.8	74.7	15.1	15.3
activation det.	19.6	226.3	38.9	50.9	15.0	16.0

3.3 Gamma spectra

Gamma spectra measured in two positions are showed in Figure 4 normalised on 1 μA. With the use of new gamma matrix, the absolute flux could be determined. The measurement 1 m from cyclotron was done during irradiation with low proton current around 3 μA and during short time, so the high energies were not measured because of low statistics. The characteristic gamma from neutron reactions, especially from capture on hydrogen and iron, can be seen. The gamma spectrum in 3 m behind shielding was measured during cyclotron operation. It has similar shape but the energies up to 18 MeV could be measured this way.

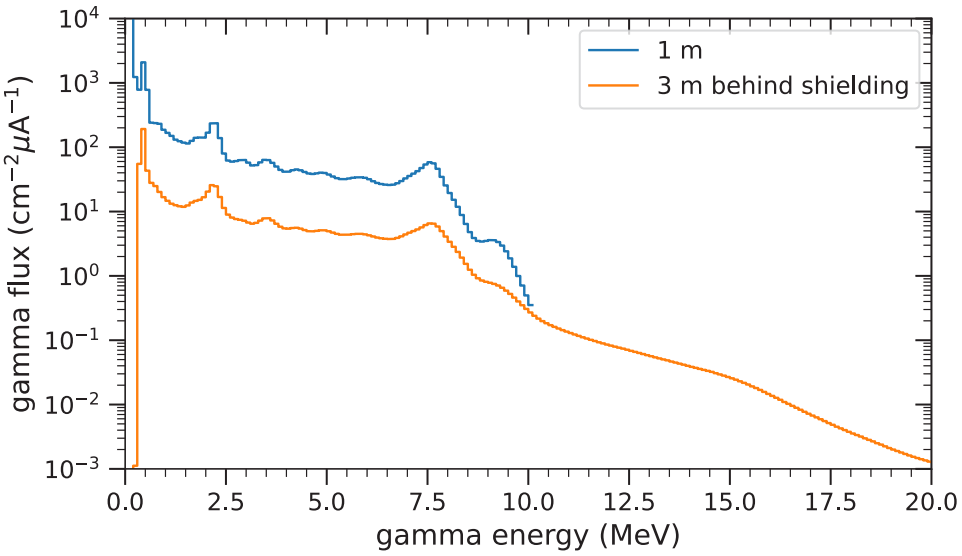

Figure 4. Gamma spectra in different positions around cyclotron.

4 Conclusion

Neutron and gamma spectra were measured around the cyclotron for production of radiopharmaceuticals. Relatively high yields of fast neutrons and gamma rays with high penetration properties were measured in both spectra. These results were confirmed by neutron activation detectors and comparison of spectral indices. It was shown that MC codes MCNP6.2 and Geant4 are insufficient in simulating the shape of the secondary neutron spectra in the basic setup, particular underestimating the fast neutron yields at back angles. The best results have been obtained in simulations with the data from EXFOR database, but these are limited only for certain angles and above the energy of 1.7 MeV. Future work will include detailed measurements of neutron spectra at various angles around a small target, as well as determination of the absolute neutron yield in the reaction of protons with enriched water.

The presented work has been realized within Institutional Support by the Ministry of Industry and Trade and with the use of the infrastructure Reactors LVR-15 and LR-0, which is financially supported by the Ministry of Education, Youth and Sports – project LM 2023041.

References

[1] M. Košťál, E. Losa, M. Schulc, J. Šimon, Z. Matěj, M. Antoš, Šimon Vadják, M. Cuhra, F. Cvachovec, F. Mravec et al., Nuclear Instruments and Methods in Physics Research, Section A: Accelerators, Spectrometers, Detectors and Associated Equipment **942** (2019)

[2] M. Košťál, M. Schulc, E. Losa, Z. Matěj, F. Cvachovec, F. Mravec, F. Brijar, T. Czakoj, J. Šimon, Šimon Vadják et al., Radiation Physics and Chemistry **184**, 109475 (2021)

[3] H.R. Vega-Carrillo, Nuclear Instruments and Methods in Physics Research Section A: Accelerators, Spectrometers, Detectors and Associated Equipment **463**, 375 (2001)

[4] R. Méndez, M.P. Iñiguez, J.M. Martí-Climent, I. Peñuelas, H.R. Vega-Carrillo, R. Barquero, Physics in Medicine and Biology **50**, 5141 (2005)

[5] A. Guimarães, M. Lacerda, J. Santos, P. Maletta, S. Rodrigues, R. Andrade, E. Vilela, T. da Silva, Applied Radiation and Isotopes **71**, 92 (2012)

[6] J. Lagares, J.G. Araque, R. Méndez-Villafañe, P. Arce, F. Sansaloni, O. Vela, C. Díaz, X. Campo, J. Pérez, Applied Radiation and Isotopes **114**, 154 (2016)

[7] D. Alloni, M. Prata, Applied Radiation and Isotopes **128**, 204 (2017)

[8] B.D. Jeffries, C. Algiere, J.A. Gallagher, T.H. Nichols, J.R. So, C.W. Littlefield, M. Quinn, J.D. Brockman, Applied Radiation and Isotopes **154**, 108892 (2019)

[9] C.J. Werner, J.S. Bull, C.J. Solomon, F.B. Brown, G.W. McKinney, M.E. Rising, D.A. Dixon, R.L. Martz, H.G. Hughes, L.J. Cox et al., *Mcnp version 6.2 release notes* (2018)

[10] M. Schulc, M. Košťál, E. Novák, R. Kubín, J. Šimon, Applied Radiation and Isotopes **151**, 187 (2019)

[11] S. Agostinelli, J. Allison, K. Amako, J. Apostolakis, H. Araujo, P. Arce, M. Asai, D. Axen, S. Banerjee, G. Barrand et al., Nuclear Instruments and Methods in Physics Research Section A: Accelerators, Spectrometers, Detectors and Associated Equipment **506**, 250 (2003)

[12] M. Hagiwara, T. Sanami, K. Masumoto, Y. Iwamoto, N. Matsuda, Y. Sakamoto, Y. Nakane, H. Nakashima, Y. Uwamino, Journal of the Korean Physical Society **59**, 2035 (2011)

[13] M. Bakhtiari, L.M. Oranj, N.S. Jung, A. Lee, H.S. Lee, Radiation Physics and Chemistry **177** (2020)
[14] A. Trkov, P. Griffin, S. Simakov, L. Greenwood, K. Zolotarev, R. Capote, D. Aldama, V. Chechev, C. Destouches, A. Kahler et al., Nuclear Data Sheets **163**, 1 (2020)
[15] D. Brown, M. Chadwick, R. Capote, A. Kahler, A. Trkov, M. Herman, A. Sonzogni, Y. Danon, A. Carlson, M. Dunn et al., Nuclear Data Sheets **148**, 1 (2018)